

Risk prevention by classical methods surveying of a bridge structure at Ségou

Prévention des risques par les méthodes classiques de la topographie d'un
ouvrage d'art à Ségou

Auteur 1 : DEMBELE Abdramane,

Auteur 2 : DEMBELE Maïchata

Auteur 3 : DIARRA Ibrahim

Auteur 4 : DAOU Ibrahima

DEMBELE Abdramane, (<https://orcid.org/0000-0001-5017-5464>*, PhD)
École Nationale d'Ingénieurs (ENI-ABT), GEC, Bamako-Mali

DEMBELE Maïchata, (Agent)
GEod Consult (GEC-MALI sarl), Bamako-Mali

DIARRA Ibrahima, (MSc)
École Nationale d'Ingénieurs (ENI-ABT), Bamako-Mali

DAOU Ibrahima, (MSc)
École Nationale d'Ingénieurs (ENI-ABT), Bamako-Mali

Déclaration de divulgation : L'auteur n'a pas connaissance de quelconque financement qui pourrait affecter l'objectivité de cette étude.

Conflit d'intérêts : L'auteur ne signale aucun conflit d'intérêts.

Pour citer cet article : DEMBELE .A , DEMBELE .M , DIARRA .I & DAOU .I (2023) «Prévention des risques par les méthodes classiques de la topographie d'un ouvrage d'art à Ségou », African Scientific Journal « Numéro 3 / Volume 17 » pp : 800 - 815

Date de soumission : Février 2023

Date de publication : Avril 2023



DOI : 10.5281/zenodo.8179149
Copyright © 2023 – ASJ



Abstract

By nature, the structures are degradable elements over time, so it is necessary to monitor these structures over time and whatever means are available to prevent the risks. What focuses this study on an auscultation through the classic measurements and careful calculations of the topography followed by analyzes in an interval of 10 months. The measurement methods are based on the survey by polar coordinates using the total station with Prism (TSP) and the survey by semi-triangulation or intersection using the total station without Prism (TSWP). The pairs of angles were observed (circle on the left and on the right) for each of the methods. The pairs of sequences, the weighted averages at the level of the coordinates and Bearings as well as statistics were calculated. The coordinates of the measurement points found down to the hundredth of a millimeter have undergone statistical processing in order to determine the errors at the temporal level at the same time as at the level of the two methods applied. Beyond that, the standard deviations were determined for possible analyses.

Keywords: auscultation, structure, surveying, standard deviations, errors

Résumé

De nature les ouvrages sont des éléments dégradables dans le temps, donc il faut un suivi temporel et travers les moyens de bords pour prévenir les risques. Ce qui focalise cette étude sur une auscultation à travers les mesures classiques et des calculs minutieux de la topographie suivis d'analyses dans un intervalle de 10 mois. Les méthodes de mesure sont basées sur le levé par coordonnées polaires à l'aide de la station totale avec prisme (TSP) et le levé par semi-triangulation ou intersection à l'aide de la station totale sans prisme (TSWP). Les paires d'angles ont été observés (cercle à gauche et à droite) pour chacune des méthodes. Les paires de séquences, les moyennes pondérées au niveau des coordonnées et Gisements ainsi que des statistiques ont été calculées. Les coordonnées des points de mesures trouvés jusqu'au centième de millimètre ont subi des traitements statistiques afin de déterminer les erreurs au niveau temporel en même temps qu'au niveau des deux méthodes sur les coordonnées. Au-delà, les ectypes ont été déterminer pour des éventuelles analyses.

Mots clés : télédétection, occupation du sol, analyse statistique, prévision, plaines

Introduction

The monitoring of a structure is based on the measurement and interpretation of physical phenomena in order to establish a diagnosis of its behavior (Boudon & Trouillet, 2011). The relevance of this diagnosis depends, to a large extent, on the quality of the monitoring measurements (Bruno, 2005; PI-BAT, 1991). In fact, incorrectly using a method or instrument can be a source of errors that can result in a wrong diagnosis (Scholtes & Leroy, 2012; Tamagnan & Beth, 2012).

Classical surveying methods are the most appropriate solutions to this problem. The bridge between Sebougouu and Bagadaji is a structure of the category “C” (the height $5 < H < 10\text{m}$) (Vidal, 2010), which has existed for many years, is located on the canal that carries wastewater to the Niger River. This bridge, which has not been inspected for a long time or even since its creation, has been the focus of a search for quality and safety of the equipment while respecting the environmental provisions (Pavaillier & Piron, n.d.). Hence the origin of our work, entitled “Risk prevention by classical methods surveying of a bridge structure at Ségou”

The present article aims to implement classical methods to see the meticulous displacement of the measurement points of the structure as well as the absolute points around.

Our research is structured as follows:

The abstract which exposes a condensed version of the whole article

The introduction which explains the subject, the context and the objective.

Material and study area: expose the different tools, and gives a detailed situation of the work.

Methodology: detail all the operations used in this work

Results: shows the different results from all the processes

Finally, we will end this article with the conclusion where we will find a confirmation of the details highlighted above.

1 Material and Study area

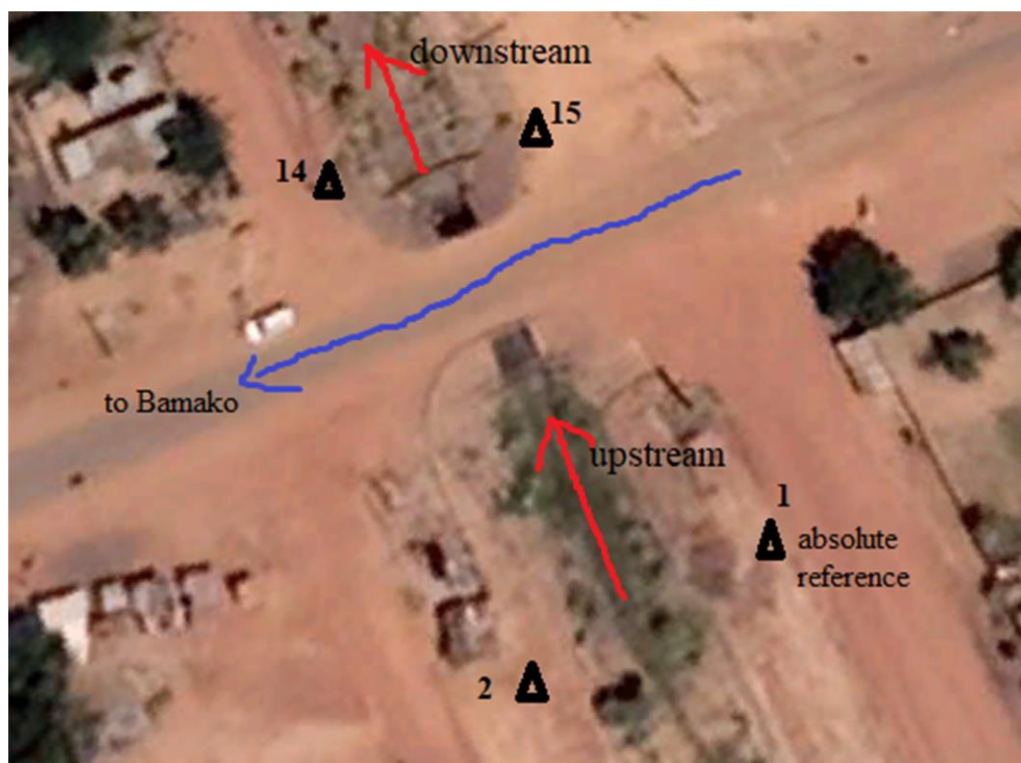
The data used are the coordinates of the two terminals S12 and S18 in UTM zone 29N. They were provided by the technical study office GEodConsult and the surveying expert office WeleTopo. The tools used are: Total station Leica, 2 rods with reflectors, a chain, markers and other accessories.

The technical operation was directed by a brigade composed of a surveyor engineer, 2 technicians and a laborer. The technical and statistical processing of the data was assured by MS Excel. Used data are:

Points	X	Y	Z
S12	791334.6391	1484667.214	300.56
S18	792823.6777	1485122.334	300.49

The study area surrounding the bridge, is located between 13°25'50" and 13°25'48" North latitude and 6°18'01" and 6°18'03" West longitude. It is located in the region of Segou in Mali precisely between Sebougou and Bagadadji, with a geology mostly made of white clay (Dembele et al., 2019). The altitude varies between 280 and 292 m.

Figure 1 Location of the bridge

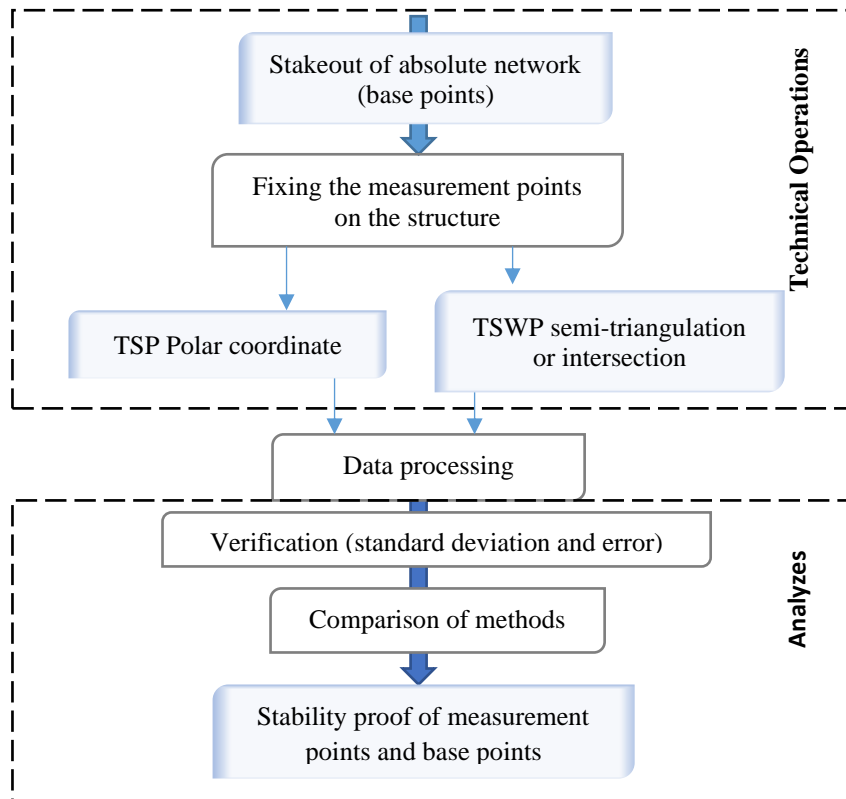


Source: google earth

2 Methodology

The methodological path is detailed by the following flow chart

Figure 2 flow chart



Source: Group Production

The process consisted of Stakeout the base points (absolute reference network) on the open position favoring the sights. Choose the measure points on the structure forming the local reference network. However, two topometric measurement methods were carried out in a series of two months each, from October 2021 to July 2022. The computed data from the two measurement methods has been used to analyze the deformation issues.

2.1 Operating mode

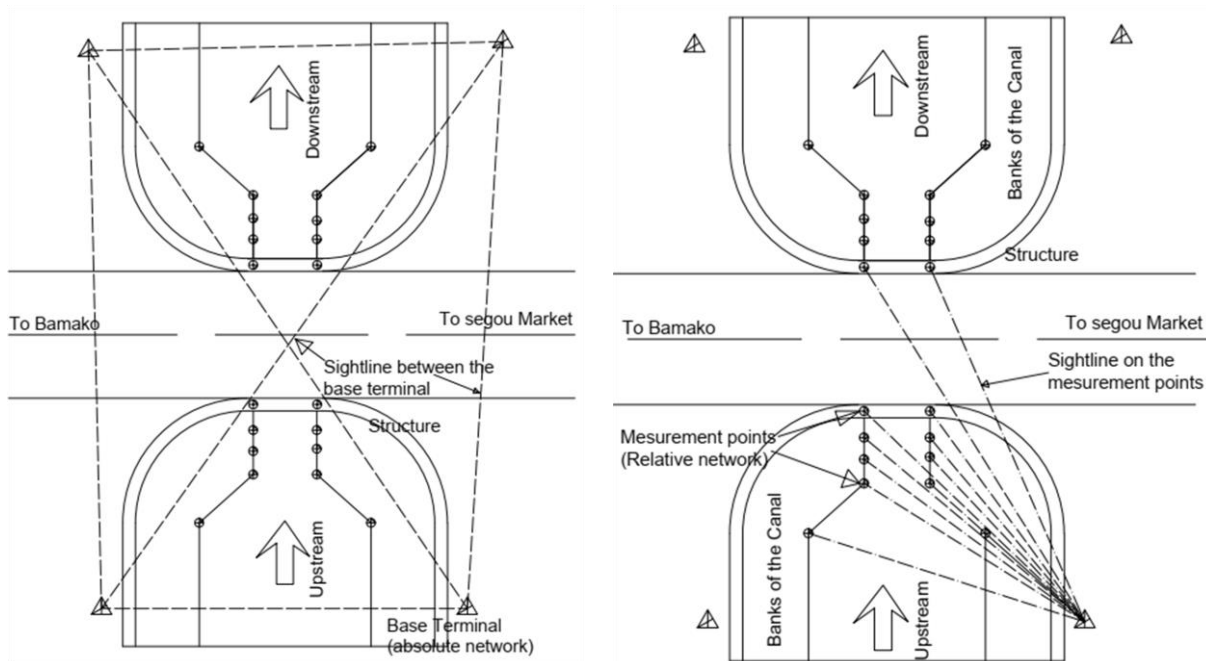
2.1.1 Staking out absolute reference network (Base points)

The absolute reference network includes an external mesh located outside the structure, from which the position of the various measurement points is determined. With such a network, we obtain the displacements of a structure in relation to its environment.

The positions of the base points have been materialized by the stakes and directly determined by a repetition of coordinates calculation during 10mn. The number of stakes is four and they

are distributed equally between upstream and downstream of the bridge i.e two for each side to get a maximum of measures (Figure 3a).

Figure 3 Different sights in the two networks



(a) Absolute network of the structure and sight

(b) Relative network of the structure and sight
12 sights per base terminal

Source: Group Production

The tridimensional coordinates of these four staked points have been determined by the GNSS measure through the DGPS while using the geodetic terminal S18 as base and S12 as control (Patil, 2020). So, the set of these points constitute our absolute reference network (Figure 3b). Our topometric observations focused both on the measurement points of the structure (network with relative measurements) and on the points of the absolute reference network.

2.1.2 Relative measures network survey (Measurement points)

Measurement points constituting the relative measures network have been surveyed by two methods which are polar coordinate and semi-triangulation. In each of the methods, each point was observed twice on the same station by applying the circle to the right and to the left of the instrument (Leica) (LAB MANUAL, 2010). This involves the calculation to eliminate horizontal and vertical collimation errors.

Overall, 20 measurement points are installed on the structure with 10 points on either side of the structure (upstream and downstream). From each station, 12 measurement points were observed, i.e 2 points on each side of the structure visible in the opposite direction in addition to the 10 points. A total of 12 sights per terminal base

Figure 4 Mesurement points of the structure



Source: Group Production

2.1.2.1 Total station with Prisms (Polar coordinate)

Basically we observed the measurement points by the measurement of angles (horizontal and vertical) and distances (Serge Milles & Lagofun, 1999). From each of the 4 stations (1, 2, 14 and 15) Figure 5, some capitals information are introduced into the memory of the station computer, such us:

- 1- Coordinates of the station and reference point noted E (east), N (north) and H (altitude).
- 2 - Station height (denoted h_i) and reflector height (denoted h_v).

During the operations we take weather conditions into account (temperature, rain, fog, refraction, etc.), and the site conditions into account (damaged or partially covered targets) to largely minimize errors.

This method was carried out on the odd account of the 10 months of auscultation, starting from the month of October, December, February, April, June.

Thus, the double and quadruple coordinates (x,y,z) of the measurement points were determined directly at each of the four terminals constituting the absolute reference network.

Figure 5 Total station Leica on the terminal base



Source: Group Production

2.1.2.2 Total station without Prisms (semi-triangulation or intersection)

Like multilateration, this second method is relatively simple to understand. But in terms of handling in the field, it requires more work because each support point is stationed and at each station a station $G0_{average}$ is calculated by the equation (1).

$$G0_{average} = \frac{\sum_{i=1}^{i=n} p_i * G0_i}{\sum_{i=1}^{i=n} p_i} \quad (1)$$

n is the number of orientation sights (number of calculated $G0_i$).

p_i represents the weight of each sight, ie its length in kilometers: $p_i = Dikm$.

In addition to the measurement of the bases at each station, we observed the horizontal and vertical angles on each of the measurement points of the structure. This is a non-contact measurement of points of the structure. The fact of not having to have prisms on the structure makes it possible to work with more safety or speed but also to avoid the intervention of mountaineers.

This method also involves measuring the height of the station and taking into account meteorological conditions and site conditions. The angles are measured by the method of the horizon survey final result of the combination of several sequences of observations (S. Milles & Lagofun, 1999; Ogundare, 2016).

2.2 Technical and statistical processing

From the so-called polar coordinate method, the coordinates of the measurement points are obtained directly during operations. Therefore, we calculated the weighted average of the coordinates on each measurement point according to the number of sights that the point received.

However, the rest of the operation was based on: the weighted average of each of the 20 measurement points obtained at each station for each of the five months (October, December, February, April, June) equation (2).

$$X_i = \frac{\sum(1/d_i * x_i)}{1/d_i} \quad Y_i = \frac{\sum(1/d_i * y_i)}{1/d_i} \quad Z_i = \frac{\sum(1/d_i * z_i)}{1/d_i} \quad (2)$$

(X_i, Y_i, Z_i) : weighted average of measurement point coordinate

d_i : horizontal distance station-measurement points

Thus, the results underwent processing and analyzes according to the appropriate tolerance to release the states of a possible settling and displacement.

Concerning the semi-triangulation method, he reiterates the same operations which constitute the sequence of operations of the polar coordinate's method. From this fact, we will specify the operation of difference-making it possible to lead to the coordinates.

The two angles linking the baseline to the measurement points being known, we proceeded to the intersection calculation to determine the coordinates of the measurement points on the structure.

Each measurement point has been pre-processed to give us the true horizontal and vertical angles. This was done with the help of the technique of the :

pair of reduced sequences of the horizontal angle equation (3)

$$Hz = \frac{Hz_{CG} + (Hz_{CD} - 200)}{2} \quad \text{if } Hz_{CD} > 200 \text{ gr}$$

$$Hz = \frac{Hz_{CG} + (Hz_{CD} - 200 + 400)}{2} = \frac{Hz_{CG} + (Hz_{CD} + 200)}{2} \quad \text{if } Hz_{CD} < 200 \text{ gr} \quad (3)$$

Hz The reduced horizontal angle

Hz_{CG} The circle to the left of the horizontal angle

Hz_{CD} The circle to the right of the horizontal angle

the average value of a vertical angle by double reversal equation (4)

$$Hv = \frac{Hv_{CG} + (400 - Hv_{CD})}{2} \quad (4)$$

Hv average value of the vertical angle

Hv_{CG} The circle to the left of the vertical angle

Hv_{CD} The circle to the right of the vertical angle

Knowing the length of the baseline, we used the equation (5) of the intersection to find the planimetric coordinates of each point:

$$Y_I - Y_A = (Y_A - Y_B) \frac{\sin(V_{BA} - V_{BI}) \cdot \cos V_{AI}}{\sin(V_{BI} - V_{AI}) \cdot \cos V_{AB}} \quad (5)$$

$$X_I - X_A = (Y_I - Y_A) \cdot \tan V_{AI}$$

(X_I, Y_I) Intersection point which is the measurement point

$(X_A, Y_A), (X_B, Y_B)$ Are the coordinates of the base points

and to determine the elevation by the generalized equation (6):

$$H_P = H_S \pm \Delta H_{(P,S)} \quad (6)$$

H_P measurement point elevation

H_S Station elevation

$\Delta H_{(P,S)}$ difference of elevation between S and P

Subsequently, the different temporal deviations as well as the standard deviations of the two methods were calculated (equation (7)) (DER Geodesie, 2020). These elements were then the subject of a detailed analysis concerning the stability of the measurement points between them and the stability of the measurement points with respect to the environment.

$$\sigma = \sqrt{\frac{\sum (x_i - \mu)^2}{N}} \quad (7)$$

σ : measurement points standard deviation

x_i : each value from the measurement points (x_i, y_i, z_i)

N : the size of the measurement points

μ : the measurement points mean

3 Results and Discussion

The obtained base points or absolute points after the measurements with the DGPS Stonex S800 are in the Table 1. The standard deviation generated by the DGPS-S800 on the control point S12 is in the order of millimeters ($\sigma_x = 0.002m$, $\sigma_y = 0.001m$, $\sigma_z = 0.003m$).

Table 1 Coordinates of the base points around the structure

Points of the absolute network	X	Y	Z
1	813834.7829	1477037.864	300.002
2	813858.0164	1477051.038	300.001
14	813863.840	1476984.029	298.795
15	813840.227	1476977.074	300.003

Source: DGPS S800 outcom

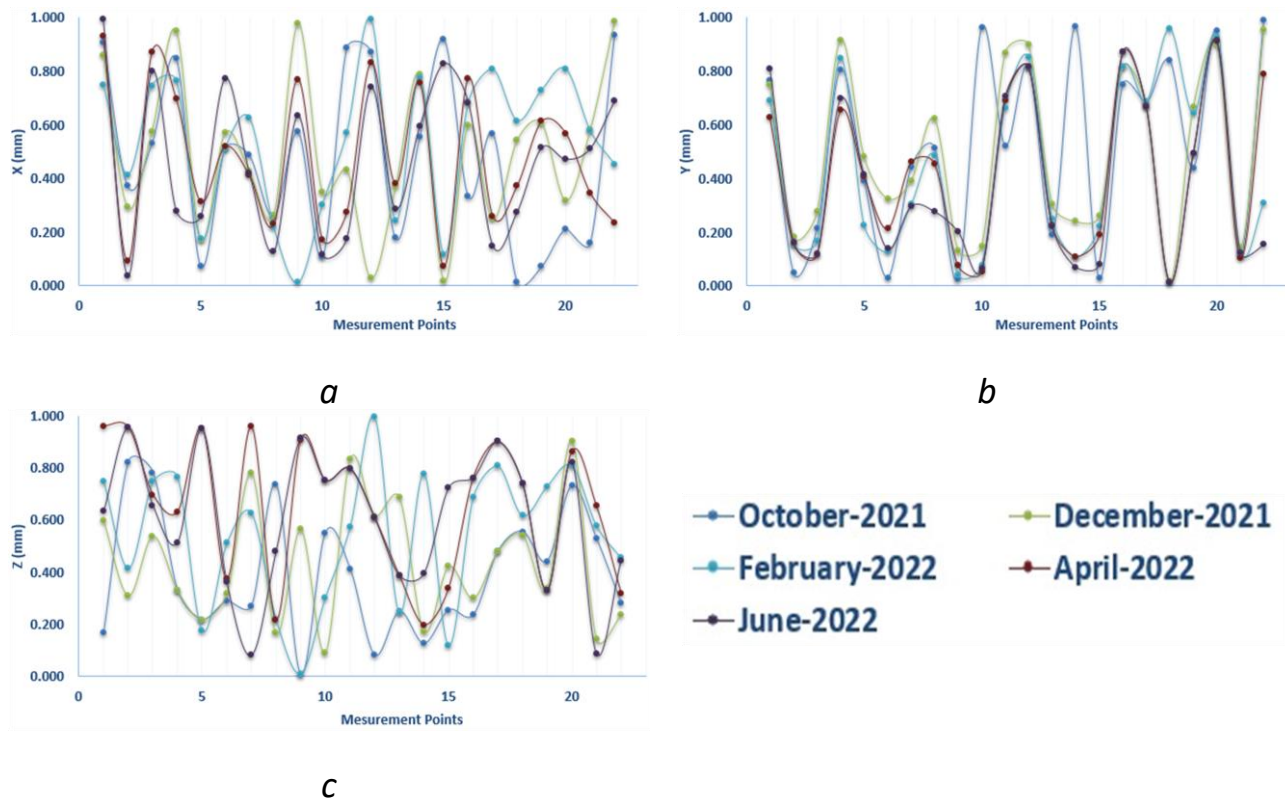
The coordinates of the points from the different methods are mostly all the same up to the centimeter level. Therefore, we perform the analysis at the millimeter level to highlight the effectiveness of the methods while identifying the displacement levels of the measurement points.

3.1 Error difference between even and odd months

Given the state of the coordinates at millimeter level on the Figure 6 and Figure 7 containing the diagrams, we observed and recorded the maximum and minimum limits on the coordinates for each month, both on the even months and odd months in the Table 2

Following the previous analyses, we have highlighted the maximums of the differences of each coordinate namely ($\Delta X(\text{mm})$, $\Delta Y(\text{mm})$, $\Delta Z(\text{mm})$) in the months according to each of the methods Table 3. The error that exists between the maximum difference of the coordinates (X, Y, and Z) of the TSP and TSWP methods shows for: X an error of $\pm 0.004\text{mm}$, Y an error of $\pm 0.008\text{mm}$, Z an error of $\pm 0.033\text{mm}$. Hence a stability of the measurement points in time. In addition to the efficiency of the methods. However these errors show the imposed advantage of the method of the Total station with Prisms (TSP) compared to the method of the Total Station without Prisms (TSWP) due to the indirect calculation of the lengths perpetrated during the calculations of the coordinates.

Figure 6 Plot of coordinates at mm level for odd months (a) X, (b) Y, (c) Z



Source: Group Production

Table 2 Limit state of coordinates on even and odd months

Total station with Prisms (Polar coordinate)					Total Station without Prisms (semi-triangulation or intersection)				
		X (mm)	Y(mm)	Z			X (mm)	Y(mm)	Z (mm)
		P22	P22	P2			P15	P18	P16
October	Max	0.936	0.989	0.821	November	Max	0.988	0.973	0.95
		P18	P9	P9			P12	P9	P9
	Min	0.014	0.024	0.007		Min	0.018	0.062	0.062
		P22	P22	P20			P4	P9	P3
December	Max	0.986	0.956	0.902	January	Max	0.811	0.968	0.904
		P15	P18	P10			P9	P10	P20
	Min	0.018	0.017	0.092		Min	0.016	0.009	0.093
		P12	P18	P12			P12	P20	P5

February	Max	0.922	0.959	0.971	March	Max	0.823	0.916	0.948
	Min	P9	P9	P12		Min	P15	P9	P16
April	Max	0.012	0.04	0.051	May	Max	0.048	0.039	0.105
		P1	P20	P1			P10	P18	P12
	Min	0.929	0.914	0.959		Min	0.996	0.990	0.954
		P15	P18	P14			P1	P3	P21
June	Max	0.073	0.012	0.197	July	Max	0.019	0.016	0.089
		P1	P20	P2			P3	P10	P9
	Min	0.993	0.909	0.954		Min	0.942	0.987	0.961
		P2	P18	P7			P15	P9	P16
		0.038	0.015	0.081			0.065	0.038	0.008

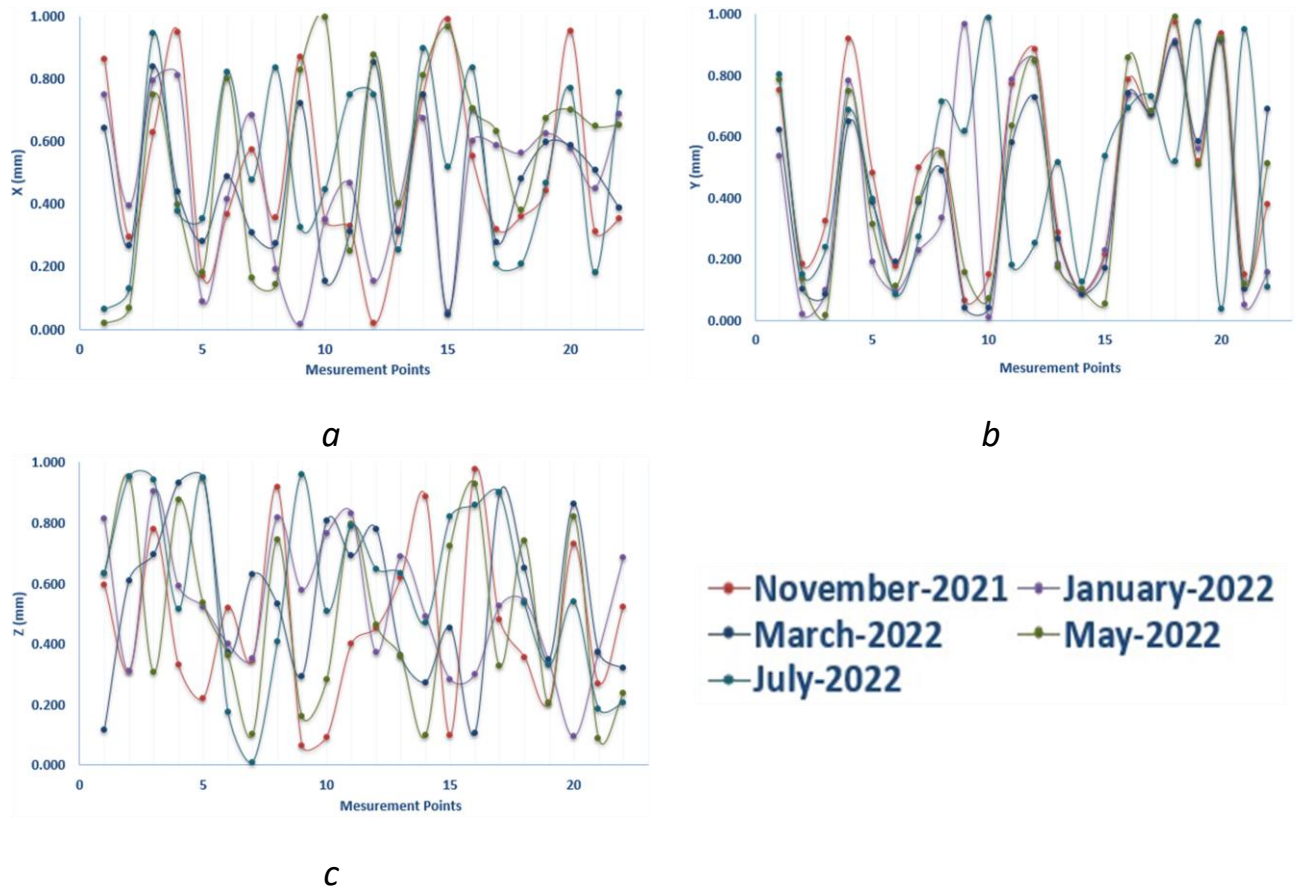
Source: Group Production

Table 3 Maximum difference on each of the coordinates in the month

Total station with Prisms (Polar coordinate)				Total Station without Prisms (semi-triangulation or intersection)			
Diff	$\Delta X(\text{mm})$	$\Delta Y(\text{mm})$	$\Delta Z(\text{mm})$	Diff	$\Delta X(\text{mm})$	$\Delta Y(\text{mm})$	$\Delta Z(\text{mm})$
Oct	0.9215	0.9658	0.8143	Nov	0.9610	0.9110	0.9132
Dec	0.9676	0.9394	0.8104	Jan	0.7948	0.9588	0.8112
Feb	0.9804	0.9190	0.9205	Mar	0.8049	0.8773	0.8431
Apr	0.8557	0.9025	0.7614	May	0.9764	0.9741	0.8652
Jun	0.9546	0.8942	0.8726	July	0.8773	0.9493	0.9532

Source: Group Production

Figure 7 Plot of coordinates at mm level for even months (a) X, (b) Y, (c) Z



Source: Group Production

3.2 Difference of error on the coordinates of the measurement points between the two methods

We can observe that the average of the differences of the maximum X ($\Delta X(\text{mm})$) of the two methods TSP and TSWP is about -0.039 mm for a standard deviation of $\pm 0.21\text{mm}$. Concerning the maximum Y ($\Delta Y(\text{mm})$), the two methods TSP and TSWP have for the average of the differences -0.036 mm for a standard deviation of $\pm 0.22\text{mm}$. The average of the maximum Z differences ($\Delta Z(\text{mm})$) is -0.002 mm for a standard deviation of $\pm 0.29\text{mm}$. This shows whatever the remote position of the stations in relation to the measurement points and whatever the classical method applied, the coordinates of the measurement points will be within the tolerance. On those, there is a stability of the structure through the measurement points.

Table 4 Standard deviation on the differences of the coordinates

MesP ts	TSP $\Delta X(\text{mm})$ Maxi	TSWP $\Delta X(\text{mm})$ Maxi	Diff	TSP $\Delta Y(\text{mm})$ Maxi	TSWP $\Delta Y(\text{mm})$ Maxi	Diff	TSP $\Delta Z(\text{mm})$ Maxi	TSWP $\Delta Z(\text{mm})$ Maxi	Diff
P1	0.9930	0.8604	0.132	0.7482	0.0193	0.728	0.2447	0.8411	-
P2	0.4137	0.3923	0.021	0.0384	0.0671	-	0.3752	0.3252	0.050
P3	0.8702	0.9425	-	0.5317	0.6279	-	0.3385	0.3145	0.024
P4	0.9489	0.9489	0	0.2789	0.3756	-	0.6700	0.5733	0.096
P5	0.3142	0.3526	-	0.0744	0.0885	-	0.2398	0.2641	-
P6	0.7723	0.8207	-	0.5102	0.3677	0.142	0.2620	0.4530	-
P7	0.6258	0.6841	-	0.4130	0.1626	0.250	0.2128	0.5214	-
P8	0.2644	0.8330	-	0.1271	0.1439	-	0.1373	0.6890	-
P9	0.9763	0.8676	0.108	0.0119	0.0162	-	0.9644	0.8514	0.113
P10	0.3477	0.9957	-	0.1071	0.1532	-	0.2406	0.8424	-
P11	0.8865	0.7473	0.139	0.1763	0.2506	-	0.7102	0.4967	0.213
P12	0.9922	0.8760	0.116	0.0295	0.0179	0.011	0.9627	0.8581	0.104
P13	0.3803	0.4020	-	0.1782	0.2530	-	0.2020	0.1490	0.053
P14	0.7865	0.8947	-	0.5560	0.6737	-	0.2305	0.2209	0.009
P15	0.9166	0.9878	-	0.0181	0.0478	-	0.8984	0.9400	-
P16	0.7738	0.8324	-	0.332	0.5505	-	0.4418	0.2819	0.159
P17	0.8060	0.6304	0.175	0.1498	0.2086	-	0.6562	0.4218	0.234
P18	0.6155	0.5607	0.054	0.0141	0.2084	-	0.6014	0.3523	0.249
P19	0.7286	0.6712	0.057	0.0717	0.4414	-	0.6568	0.2297	0.427
P20	0.8075	0.9497	-	0.2127	0.5751	-	0.5948	0.3745	0.220
P21	0.5811	0.6476	-	0.1586	0.1811	-	0.4225	0.4664	-
P22	0.9857	0.7555	0.230	0.2358	0.352	-	0.7498	0.4035	0.346
	Average		-	Average		-	Average		-
	Standard		0.209	Standard		0.218	Standard		0.287

Source: Group Production

Overall, the errors show maximum displacements in the order of tenths of a millimeter for each method. This indicates a stability of the measurement points on the structure and the absolute network points around the structure. Hence both methods are able to follow the evolution of a structure or a fault in time.

Conclusion

Auscultation of Structures through the classic methods of topography, implemented with the necessary rigor and modern calculation means, makes it possible to provide reliable and comparable displacement measurements from one control campaign to another. These methods of measurement, although less precise than other types of measurement, for example the lasergrammetry, the movements of pendulums, have the great advantage of providing measurements of the individual movements of the measurement points on the structure and even of the site if the latter are instrumented. In addition, topometric auscultation provides very significant 3D movements for understanding the interaction of movements on complex civil engineering structures.

The contribution of these high-precision coordinate measurement methods makes it possible to significantly improve the reliability of the results while reducing the number of observation stations and thereby increasing the efficiency of the work.

The application of methodologies by polar coordinates and by semi-triangulation or intersection as well as the processing of data for the Ségou bridge has made it possible to highlight the effects of reinforcement. The analysis of the results showing errors and minimal standard deviations, indicates a stability of the structure both at the planimetric and altimetric level.

BIBLIOGRAPHIE

- Boudon, R., & Trouillet, M. (2011). La surveillance des ouvrages à EDF. *Revue XYZ*, 128, 25–32.
- Bruno, G. (2005). Les Techniques d'auscultation des ouvrages en Béton Armé. *Association Francaise de Genie-Civil*, 1–57.
- Dembele, A., Xiufen, Y., Adama, M., & Daou, I. (2019). Topography State analysis using structures. *Proceedings of 2019 IEEE International Conference on Mechatronics and Automation, ICMA 2019*, 480–484. <https://doi.org/10.1109/ICMA.2019.8816479>
- DER Geodesie. (2020). Theorie des erreurs et Compensation. *ENI-ABT-MALI*, 1–80.
- LAB MANUAL. (2010). SURVEYING - II. *Aurora's Technological & Research Institute*, 1–83.
- Milles, S., & Lagofun, J. (1999). Topographie et topométrie modernes. *Toponet-Geod*, 5(2), 1–526.
- Milles, Serge, & Lagofun, J. (1999). Topographie et topométrie modernes: Techniques de mesure et de représentation (1). *Toponet-Geod*, 5(1), 1–300.
- Ogundare, J. O. (2016). Precise surveying. *Wiley Publishing, Inc*, 1–714. <http://library.iyte.edu.tr/tezler/master/makinamuh/T000703.pdf>
- Patil, V. (2020). DGPS BASED DIGITAL TOPOGRAPHIC SURVEY. *ICRTET - 2018, December*, 901–907.
- Pavaillier, F., & Piron, A. (n.d.). *Auscultation des ouvrages de Génie Civil Maitrise de la qualité de la mesure Monitoring of civil engineering structures Quality control of measurement*. 1–9.
- PI-BAT. (1991). *Techniques d'auscultation des ouvrages de génie civil*. 193.
- Scholtes, P., & Leroy, R. (2012). Concept de l'auscultation topométrique de la théorie à la pratique. *Comité Français Des Barrages et Réservoirs*, 1–16.
- Tamagnan, D., & Beth, M. (2012). Etat de l'art des techniques récentes en auscultation topographique. *Colloque CFBR, Auscultation Des Barrages et Des Dignes, Pratiques et Perspectives*, 1–14.
- Vidal, R. (2010). *Auscultation d'ouvrages hydrauliques*.